Modification of MCM-48-, SBA-15-, MCF-, and MSU-type Mesoporous Silicas with Transition Metal Oxides Using the Molecular Designed Dispersion Method

Piotr Kuśtrowski,*,† Lucjan Chmielarz,† Roman Dziembaj,† Pegie Cool,‡ and Etienne F. Vansant‡

Faculty of Chemistry, Jagiellonian University, Ingardena 3, 30-060 Kraków, Poland, and Laboratory of Adsorption and Catalysis, Department of Chemistry, University of Antwerp, Universiteitplein 1, 2610 Wilrijk, Belgium

Received: February 8, 2005; In Final Form: April 21, 2005

Four various mesoporous silicas (MCM-48, SBA-15, MCF, and MSU) were modified by the molecular designed dispersion method using $Fe(acac)_3$, $Cr(acac)_3$, and $Cu(acac)_2$ complexes. The deposition was performed at the same concentration of the metal acetylacetonate (acac) complex in a toluene solution. All as-synthesized samples were investigated by diffuse reflectance infrared Fourier transform spectroscopy, Fourier transform infrared photoacoustic spectroscopy, and thermogravimetric analysis. The calcined materials were studied with respect to their textural properties (Brunauer−Emmett−Teller adsorption isotherm) and chemical composition (electron microprobe analysis). It allowed elucidation of the mechanism of interaction between the acac complex and the silanol groups. For the MCM-48, SBA-15, and MCF materials, the formation of hydrogen bonding was found for the chromium- and copper-modified samples, whereas the Fe-containing materials showed the ligand exchange mechanism. The strong interaction of the MSU support and the different acetylacetonate complexes, resulting in a loss of at least one acac ligand, was observed. The mesoporous silicas modified with transition metal oxides were studied by UV−vis−DR spectroscopy. The different metal dispersions were found for the samples containing various transition metal oxides.

Introduction

Ordered mesoporous silicas, which were first synthesized by scientists from Mobil,[1,2] possess high surface area and uniform porous structure and therefore are desirable for catalytic and adsorption processes involving large molecules. Micelle templated structures (MTS) can be synthesized using different types of templates. The positively charged surfactants (e.g. quaternary ammonium ions) were proposed for the synthesis of MCM-41, MCM-48, and MCM-50.[1,2] Recently, high-quality MCM-48 was prepared using cationic Gemini surfactants C_{n-s-n} with $n = 16$, 18, or 22 and the spacer having 10 or 12 carbons ($s = 10$ or 12).[3−5] SBA-15-type silicas are obtained in the presence of nonionic surfactants. The formation of SBA-type materials is a result of interaction of amphiphilic block copolymer ($EO_xPO_yEO_x$) and inorganic siliceous species through hydrogen bonding.[6,7] The synthesis is performed under acidic conditions. At low pH, the hydrophilic headgroups (EO units) and the positively charged silica species are assembled together by electrostatic interactions mediated by the negatively charged chloride ions. By changing the size of the EO group, the materials differ in the pore diameter (up to 30 nm). However, the most important advantage of SBA-type materials is the thickness of their walls, which are significantly thicker compared to those of the MCM-type silicas.

It was shown[8−10] that adding a hydrophobic swelling agent (e.g. 1,3,5-trimethylbenzene, xylene) during the synthesis of SBA-15 induces a phase transformation from the highly ordered hexagonal (*P*6*mm*) symmetry to mesostructured cellular foam (MCF) composed of uniformly sized, large spherical cells that are interconnected by uniform windows. The pores constitute a 3D channel system, where the channels have a significant larger diameter compared to that of SBA-15. Therefore, MCF seems to be a very promising candidate for catalytic supports. Recently, Han et al.[11] showed that enzymes (e.g. versatile enzyme) can be successfully immobilized in mesocellular siliceous foam, and the large porosity of support provides a better access for the reactants to the active sites.

The electrically neutral S^0I^0 assembly pathway was also used by Pinnavaia and co-workers[12−14] for the synthesis of MSU-type materials. They exhibit a porous 3D-wormhole-like structure and large particle sizes.

The attractiveness of mesoporous silicas as potential catalysts can be enhanced by a modification of their surface with transition metal oxides. The method of active-phase introduction is a crucial parameter influencing the catalytic activity. Grafting using metal complexes seems to be a very promising method of transition metal oxide deposition, which allows controlling the creation of the active centers on a nanoscale.[15−17] In such a case, the uniform distribution of the metal complexes over the support surface can be achieved by using specific functional groups on the surface. The surface hydroxyls or silanols can play a role of anchoring point for the reacting metal complexes.

In the late 1980s and the beginning of the 1990s the dispersion of acetylacetonate (acac) complexes was carried out on silica and alumina surfaces.[15,18−21] Metal acetylacetonates used in grafting have some advantages. The large acac ligands reduce the probability of metal clustering, as the metal atoms are kept far away from each other. Furthermore, acetylacetonate complexes are less moisture-sensitive. For example, $Cu(acac)_2$,[22]

* To whom correspondence should be addressed. Tel.: +48 12 6632006; Fax: +48 12 6340515; E-mail: kustrows@chemia.uj.edu.pl.
† Jagiellonian University.
‡ University of Antwerp.

10.1021/jp050696o CCC: $30.25
Published on Web 05/21/2005

$VO(acac)_2$,[23] $MoO_2(acac)_2$,[24] $TiO(acac)_2$,[25] $Cr(acac)_3$,[26] and $Fe(acac)_3$[27] were successfully dispersed on the silica support. This kind of grafting is known as molecular designed dispersion (MDD). The detailed studies of the MDD method showed that there are two possible ways of interaction between the acac complex and the hydroxyl groups of the silica support. The first mechanism involves a hydrogen bonding between the pseudo π system of the acac ligand and the proton of the silanol group. However, the interaction by a ligand exchange with the formation of a covalent $Me-O_{support}$ bond is also possible. In the subsequent step to the grafting, the adsorbed complex is thermally decomposed with a mild oxidation procedure to obtain a transition metal oxide supported on the surface.

In this paper we discuss the mechanism of $Fe(acac)_3$, $Cr(acac)_3$, and $Cu(acac)_2$ deposition on the mesoporous silica (MCM-48, SBA-15, MCF, and MSU) supports studied by thermogravimetric and spectroscopic methods. Furthermore, the influence of textural parameters of parent material on the metal oxide loading was investigated.

Experimental Section

For synthesis of MCM-48, 2.89 g of a $C_{16-12-16}$ Gemini and 0.35 g of NaOH were dissolved in 60.0 mL of distilled water and stirred until the surfactant was dissolved.[3] Then, 2 g of fumed silica (Aerosil 380) was added under vigorous stirring. After 30 min of mixing at room temperature, the resulting gel was transferred into an autoclave and aged at 130 °C for 3 days. Subsequently, it was filtered, washed with 30 mL of distilled water, and resuspended in distilled water (30 mL) for 24 h at 130 °C. This procedure was carried out twice. The final product was separated by filtration, washed with distilled water, and dried at room temperature.

Mesoporous silica SBA-15 was synthesized according to the procedure described earlier by Van Bavel et al.[28] A 4.0 g amount of poly(ethylene oxide)-*block*-poly(propylene oxide)-*block*-poly(ethylene oxide) triblock copolymer ($EO_{20}PO_{70}EO_{20}$, Pluronic P123) was dissolved in 1.6 M HCl (150 mL), and then 9.14 mL of tetraethyl orthosilicate (TEOS) was added. The obtained suspension was stirred at 45 °C for 8 h and then aged at 80 °C for 15 h. The solid product was filtered, washed with distilled water, and dried at room temperature.

The synthesis method of MCF was given previously by Schmidt-Winkel et al.[8] A 4.0 g amount of Pluronic P123 was dissolved in 150 mL of aqueous HCl solution (1.6 M) at 35−40 °C. Then, NH_4F (46.7 mg) and 1,3,5-trimethylbenzene (mesitylene, 2.0 g) were added and vigorous stirred for 1 h. Subsequently, tetraethyl orthosilicate (TEOS, 9.14 mL) was added. After 20 h at 35−40 °C, the slurry was transferred to an autoclave and aged at 100 °C for 24 h. The obtained precipitate was filtered, washed with distilled water, and dried in air.

The synthesis of MSU was performed using a modified procedure described by Kim et al.[29] Sodium silicate (11.8 mL) was dissolved in 278 mL of distilled water and mixed with 0.22 M brij 56 (5.5 mL) and acetic acid (2.5 mL). After 1 h, NaF (0.06 g) was added, and the resulting gel was left at 60 °C for 3 days under vigorous stirring. Finally, the white product was filtered, washed with distilled water, and dried at room temperature.

Prior to the modification with transition metal complexes, the samples were calcined at 550 °C with a heating rate of 1 °C/min and an isothermal period of 8 h in air. Deposition of metal acetylacetonates ($Fe(acac)_3$, $Cr(acac)_3$, and $Cu(acac)_2$) was performed by the liquid-phase molecular designed dispersion (MDD) method in a dry nitrogen glovebox. A 1 g amount of the thermally treated support was stirred at room temperature (for $Fe(acac)_3$ and $Cr(acac)_3$) or at 50 °C (for $Cu(acac)_2$) in a zeolite-dried toluene (100 mL) containing 0.4 mmol of metal acetylacetonate. The deposition of Cu acetylacetonate was performed at the higher temperature due to a limited solubility of this complex in toluene. The contact time during the reaction between the metal acetylacetonate complex and the support was 1 h. The modified support was filtered and washed five times with fresh solvent in order to remove the excess of the metal acac complex. A washing cycle consisted of washing 1 g of the deposited sample with an aliquot of 25 mL of toluene.[22] The sample was dried under vacuum at room temperature. Finally, the material was calcined at 550 °C with a heating rate of 1 °C/min and an isothermal period of 8 h in air atmosphere.

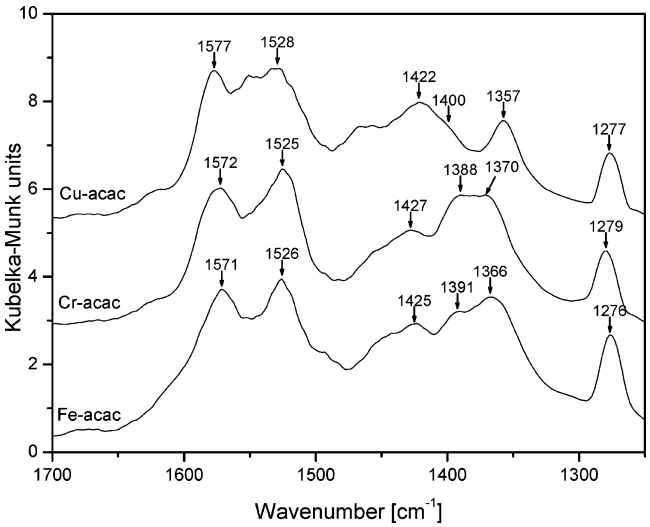

Figure 1. Diffuse reflectance FTIR spectra of bulk $Fe(acac)_3$, $Cr(acac)_3$, and $Cu(acac)_2$.

Transition metal oxide loadings were determined by electron microprobe analysis performed on a JEOL Superprobe 733. Thermogravimetric measurements were performed on a Mettler TG50 thermobalance, equipped with an M3 microbalance and connected to a TC10A processor. Samples were heated in an oxygen flow from 50 to 550 °C at a rate of 5 °C/min. Textural parameters of the samples were determined by N_2 sorption at −196 °C using an ASAP 2010 (Micromeritics) after outgassing the materials under vacuum at 200 °C for 16 h. DRIFT spectra were recorded on a Nicolet 20SXB FTIR spectrometer equipped with a Spectra-Tech diffuse reflectance accessory. The resolution was 4 cm^{-1}, and 200 scans were collected for a 2 wt % diluted sample in KBr. The photoacoustic IR spectroscopy (PAS) was performed on a Nexus spectrometer bench placed in an ultradry air box and equipped with a MTEC 300 PA detection cell flushed with zeolite-dried helium. 2000 scans were usually taken with a resolution of 4 cm^{-1}. UV−vis diffuse reflectance (UV−vis−DR) analysis was carried out on a Nicolet Evolution 500 spectrophotometer. The spectra were taken in the range of 200−800 nm for the samples (2 wt %) diluted in KBr.

Results and Discussion

The diffuse reflectance infrared Fourier transform (DRIFT) spectra of bulk $Fe(acac)_3$, $Cr(acac)_3$, and $Cu(acac)_2$ are presented in Figure 1, while the diffuse reflectance FTIR spectra of the SBA-15 sample, before and after contact with a solution of metal acetylacetonate complex in toluene followed by washing and drying, are shown in Figure 2. The appearance of bands characteristic for the acetylacetonate ligands was found after

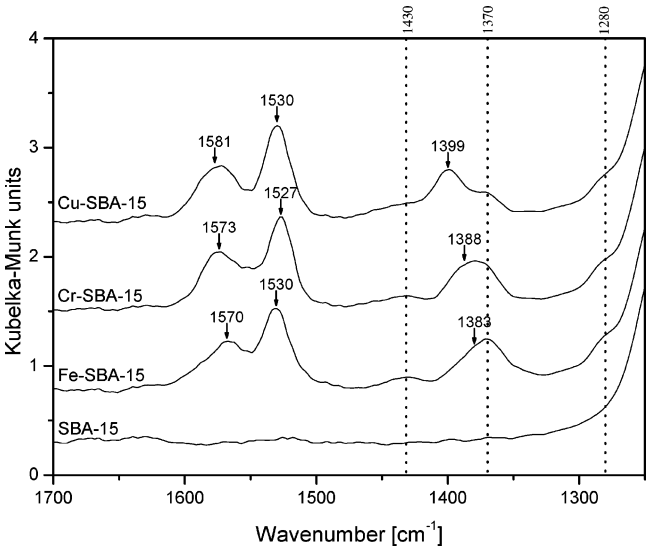

Figure 2. Diffuse reflectance FTIR spectra of nonmodified SBA-15 support and SBA-15 sample after modification with $Fe(acac)_3$, $Cr(acac)_3$, and $Cu(acac)_2$.

the modification of mesoporous silicas with the acac complexes. The position of the bands in the region of the acac ligands vibrations (1250−1600 cm^{-1}) is similar for the bulk metal acetylacetonate and the samples modified with this acac complex (cf. Table 1). Nevertheless, the influence of support and the central metal ion of the complex on the C−O and C−C absorption bands can be observed. These effects are the most distinct in the case of $\nu_s(C-O)_{ring}$ and $\nu_{as}(C-O)_{ring}$ stretching vibrations. The $\nu_s(C-O)_{ring}$ stretching vibration is typically situated in the range of 1570−1572, 1573−1577, and 1581−1582 cm^{-1}, whereas for the $\nu_{as}(C-O)_{ring}$ 1382−1384, 1387−1389, and 1399−1402 cm^{-1} for the different supports after the reaction with $Fe(acac)_3$, $Cr(acac)_3$, and $Cu(acac)_2$, respectively, can be observed. However, the positions of the $\nu_s(C-O)_{ring}$ and $\nu_{as}(C-O)_{ring}$ vibrations for the acac complexes deposited on MSU differ significantly from those recorded in the case of other samples. There is no significant difference in the position of the vibration of carbon−carbon double bonds in the conjugated chelate rings coordinated to the metal ion. The $\nu_{as}(C-C-C)_{ring}$ stretching vibration is positioned in the range of 1527−1532 cm^{-1} for all samples. Moreover, the DRIFT spectra of the samples modified with the acac ligands show weak bands at around 1430, 1370 and 1280 cm^{-1}, which can be attributed to the vibrations of C−H bonds.[26,28]

The interaction of the acetylacetonate complexes with the surface of the mesoporous supports was also followed by photoacoustic infrared spectroscopy (PAS). The FTIR-PAS spectra recorded for the calcined and modified supports are presented in Figure 3. The spectrum of nonmodified mesoporous silicas pretreated at 550 °C shows the strong band at 3745 cm^{-1}, assigned to the free OH vibration, and a broad band between 3600 and 3200 cm^{-1}, attributed to the vibration of polydentate hydroxyl functional groups. After the reaction with the acac complexes followed by washing and drying, the intensity of the band at 3745 cm^{-1} decreased, indicating that a part of the isolated hydroxyls disappeared. Simultaneously, an increase in the very broad absorption band around 3300−3500 cm^{-1}, which is associated with hydroxyls being in hydrogen bond interactions, is found. This effect is the least distinct for the MSU sample modified with the acac complexes (Figure 3D). At the same time, the acetylacetonate vibration bands in the 1300−1600 cm^{-1} region (discussed previously) appear, pointing toward the high amount of acac complex grafted on the surface of mesoporous silicas.

The reaction mechanism of the acac complexes with the support surface can be determined by the calculation of the ratio *R*:

$$R = \frac{(\text{mmol of acac})/(\text{g of support})}{(\text{mmol of Me})/(\text{g of support})}$$

The amount of acac ligands present on the surface of materials modified with the acac complexes was determined by measuring the weight loss in an oxygen flow, whereas the content of transition metals in the deposited samples was obtained by chemical analysis. The results are collected in Table 2. For the MCM-48, SBA-15, and MCF supports modified with $Cr(acac)_3$ and $Cu(acac)_2$, the *R*-value is found to be very close to the number of acetylacetonate ligands present in the parent complex. It should be therefore concluded that the Cu and Cr acetylacetonate complexes interact with the surface of these mesoporous silicas by hydrogen bonding. A different effect is observed for the MCM-48, SBA-15, and MCF materials modified with $Fe(acac)_3$. These samples show the *R*-value of 2.0, indicating the ligand-exchange mechanism for the $Fe(acac)_3$ complex. Such a mechanism is understandable due to the low stability of the iron acetylacetonate, which easily loses the acac ligands.[30] The lower *R*-values for the MSU-based materials reveal that the interaction of $Cr(acac)_3$ and $Cu(acac)_2$ with the surface occurs in two different ways. Part of the metal complex reacts with silanol groups present in MSU via the ligand-exchange mechanism with the formation of a M−O−Si bonding and a loss of acac ligand. For the $Cr(acac)_3$ and $Cu(acac)_2$ complexes, however, a hydrogen bonding with the surface hydroxyls, comparable with MCM-48, SBA-15, and MCF materials can also be assumed. The *R*-value of 1.2 found for the Fe-MSU sample suggests the abstraction of two acac ligands from the $Fe(acac)_3$ complex with the formation two Fe−O− support bondings, in which two adjacent silanol groups take part. The different mechanism of interaction between acac complexes and the surface of MSU could suggest a more Broensted acidic nature or/and a higher density of silanol groups present on the surface compared to the MCM-48, SBA-15-, and MCF-type mesoporous silicas.

The calcination of the modified supports containing differently bonded metal acac species in an oxygen-containing atmosphere results in a gradual decomposition of organic surface species (Figure 4). The mesoporous silicas, supported with $Fe(acac)_3$, decompose starting from about 100 °C and show three clearly separated weight losses around 160−170, 230−240, and 300−305 °C. The stronger interaction of iron acetylacetonate with the MSU surface results in a shift in the decomposition process toward higher temperatures. In this case, the following stages in the decomposition can be found around 200, 250, and 315 °C, respectively. The samples modified with $Cr(acac)_3$ appear to be more stable compared to the Fe-containing materials. This effect should be attributed to the higher thermal stability of the $Cr(acac)_3$ complex. As shown in Figure 4B, the decomposition of the Cr-doped MCM-48, SBA-15, and MCF samples begins at about 140 °C and follows by two (for Cr−SBA-15 and Cr−MCF) or three stages (for Cr−MCM-48). Cr−SBA-15 and Cr−MCF show differential thermogravimetric (DTG) peaks around 205 and 310 °C, while Cr−MCM-48 reaches the maximum rate of decomposition around 195, 245, and 315 °C, respectively. A significantly different profile of the DTG curve is observed for Cr−MSU. This sample starts to decompose at temperature as low as 120 °C; however, it shows

TABLE 1: Assignment of Vibrations Observed in the DRIFT Spectra of Mesoporous Materials Modified with $Fe(acac)_3$, $Cr(acac)_3$, and $Cu(acac)_2$

	wavenumber (cm^{-1})					
sample	$\nu_s(C-O)_{ring}$	$\nu_{as}(C-C-C)_{ring}$	$\delta_{as}(C-H)$	$\nu_{as}(C-O)_{ring}$	$\delta_s(C-H)$	$\nu_s(C-C-C)_{ring}$
bulk $Cu(acac)_2$	1577	1528	1422	1400	1357	1277
Cu−MCM-48	1582	1530	1433	1402	1370	1279
Cu−SBA-15	1581	1530	1429	1399	1370	1278
Cu−MCF	1581	1529	1434	1399	1373	1281
Cu−MSU	1587	1529	1433	1399	1372	1280
bulk $Cr(acac)_3$	1572	1525	1427	1388	1370	1279
Cr−MCM-48	1577	1527	1436	1389	1374	1280
Cr−SBA-15	1573	1527	1432	1388	1372	1278
Cr−MCF	1575	1528	1433	1387	1373	1281
Cr−MSU	1577	1527	1428	1394	1375	1278
bulk $Fe(acac)_3$	1571	1526	1425	1391	1366	1276
Fe−MCM-48	1571	1532	1435	1384	1370	1279
Fe−SBA-15	1570	1530	1432	1383	1368	1278
Fe−MCF	1572	1530	1432	1382	1367	1279
Fe−MSU	1589	1529	1429	1394	1373	1279

TABLE 2: Chemical Analysis of Supports Modified with Metal Acetylacetonate Complexes and Textural Parameters of Materials after Calcination

	metal loading						
sample	mmol/g	μmol/m^2	acac loading (mmol/g)	*R*-value	surface area (m^2/g)	total pore vol (cm^3/g)	av pore diam (Å)
MCM-48					909	1.08	36
Fe−MCM-48	0.29	0.34	0.58	2.0	850	0.98	36
Cr−MCM-48	0.21	0.25	0.60	2.9	852	1.01	36
Cu−MCM-48	0.18	0.21	0.38	2.1	842	1.01	36
SBA-15					773	0.85	78
Fe−SBA-15	0.31	0.41	0.62	2.0	764	0.85	78
Cr−SBA-15	0.18	0.24	0.50	2.8	735	0.82	78
Cu−SBA-15	0.31	0.41	0.55	1.8	759	0.84	78
MCF					698	2.35	260
Fe−MCF	0.31	0.49	0.61	2.0	629	2.20	260
Cr−MCF	0.16	0.25	0.46	2.9	630	2.29	260
Cu−MCF	0.27	0.46	0.50	1.9	593	2.24	260
MSU					271	0.78	∼100
Fe−MSU	0.39	1.51	0.46	1.2	259	0.72	∼100
Cr−MSU	0.12	0.82	0.29	2.4	147	0.44	∼100
Cu−MSU	0.22	1.00	0.30	1.4	219	0.69	∼100

the highest rate of decomposition around 260 and 315 °C. The Cu-containing MCM-48, SBA-15, and MCF samples (cf. Figure 4C) are decomposed in two essential steps around 200 and 250 °C. Similarly to Fe- and Cr-modified MSU, also Cu−MSU shows a different mechanism of the decomposition compared to that of Cu−MCM-48, Cu−SBA-15, and Cu−MCF. Only one DTG peak is observed in the temperature range characteristic of acac complexes decomposition. It should be, however, concluded that, regardless of the difference in the mechanism decomposition, the mesoporous silica supports modified with the acac complexes after the thermal treatment at 550 °C form the corresponding supported transition metal oxide materials.

The textural properties of the parent and modified MCM-48, SBA-15, MCF, and MSU are summarized in Table 2. The MCM-48 sample calcined at 550 °C has a Brunauer−Emmett−Teller (BET) surface area of 909 m^2/g, a total pore volume of 1.08 cm^3/g, and an average pore diameter of 36 Å. A BET surface area of SBA-15, MCF, and MSU is 773, 698, and 271 m^2/g, with a total pore volume of 0.85, 2.35, and 0.78 cm^3/g and an average pore diameter of 78, 260, and 100 Å, respectively. An introduction of transition metal oxides onto the surface of the molecular sieves results in a slight decrease in the surface area as well as the total pore volume. This effect is the most pronounced for the Cu- (Cu−MCM-48 and Cu−MCF) and Cr-containing (Cr−SBA-15 and Cr−MSU) samples. It should be, however, stressed that the rather low concentration of acac solution applied during the deposition process does not cause significant pore blocking effects.

The calcined samples differ in the content of transition metals (cf. Table 1). It should be noticed that the metal loading depends strongly on the kind of acac complex used in the MDD method. The deposition procedure used enables one to introduce the highest amount of iron. This effect should be assigned to the ligand-exchange mechanism of interaction of $Fe(acac)_3$ with the support surface. The lowest content of transition metal was obtained after the modification of the supports with $Cr(acac)_3$. This should be explained by the hydrogen bonding interaction of chromium acetylacetonate complex with the surface hydroxyls. On the other hand, the $Cr(acac)_3$ complex possesses the octahedral arrangements of the oxygen atoms around the central metal ion, which can lead to steric effect in a transportation of the acac complex to the internal surface. When the metal loading is related to the BET surface area of the samples, the influence of the porosity on the Fe, Cr, and Cu content is clearly observed (cf. Table 2). The smallest amount of transition metals was deposited on the MCM-48 samples due to very narrow pores present in this material. An increase in the pore size results in raising the metal loading obtained in the calcined sample. The relatively highest surface content of the transition metal is found for the MSU materials—1.51 μmol Fe/m^2 Fe−MSU, 0.82 μmol Cr/m^2 Cr−MSU, and 1.00 μmol Cu/m^2 Cu−MSU.

The diffuse reflectance UV−vis spectra were recorded for the calcined samples in order to study the coordination environment of transition metals. The examples of UV−vis spectra recorded for the calcined SBA-15-based samples are shown in Figure 5. The spectra of pure supports show only a very weak

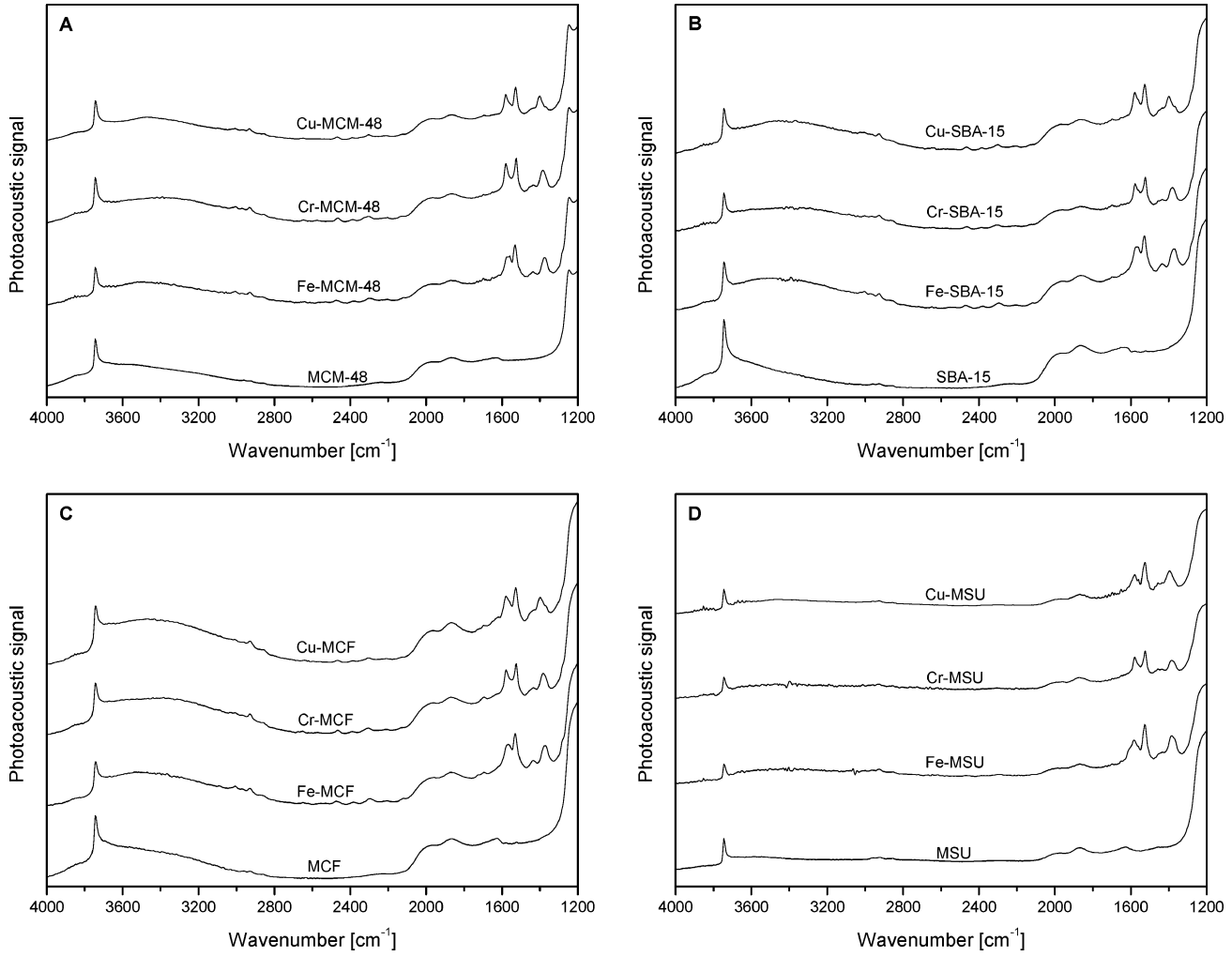

Figure 3. Infrared photoacoustic spectra of nonmodified mesoporous supports and the samples after modification with $Fe(acac)_3$, $Cr(acac)_3$, and $Cu(acac)_2$.

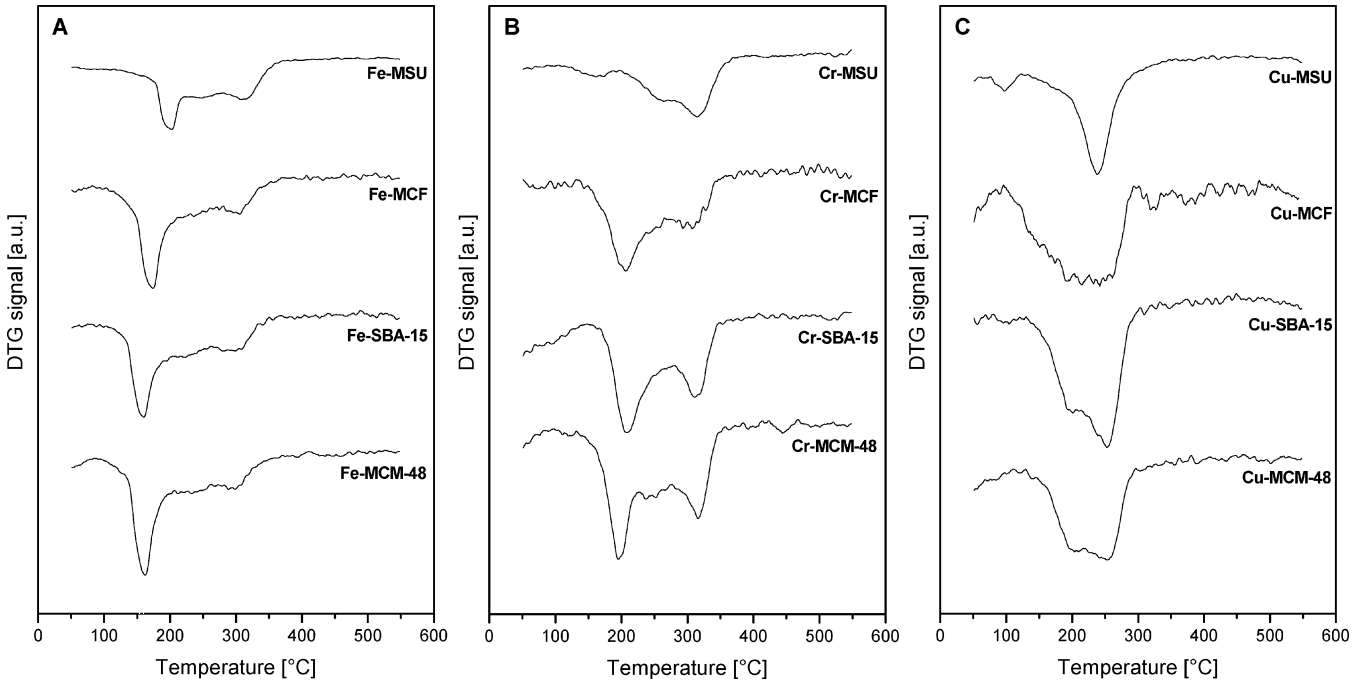

Figure 4. DTG profiles for mesoporous silicas modified with Fe (A), Cr (B), and Cu (C).

band centered at 250−270 nm attributed to structural Si in tetrahedral coordination. After the modification with Fe, the intense band centered at about 260 nm, corresponding to the $d\pi-p\pi$ charge transfer between iron and oxygen atoms in

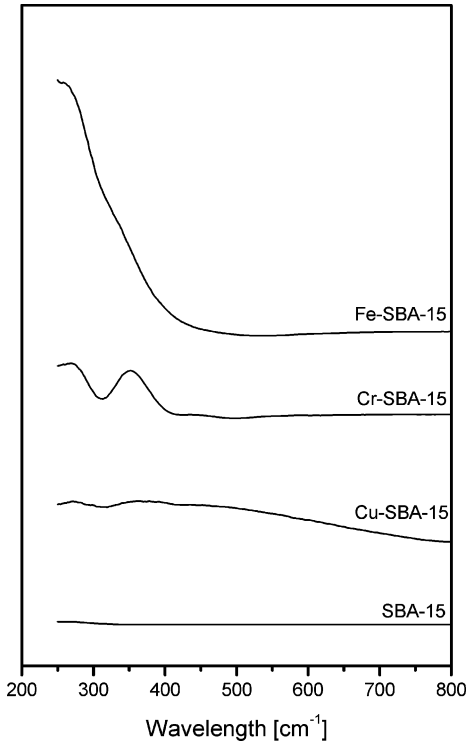

Figure 5. UV−vis diffuse reflectance spectra of calcined SBA-15 samples nonmodified and modified with transition metal oxides.

isolated Fe^{3+} species, appears. Moreover, the weak band in the range of 300−450 nm, attributed to small oligonuclear $(FeO)_n$ species,[31,32] can be distinguished. It should be noticed that the relation between the amount of isolated and oligonuclear species, estimated on the basis of determined peak areas, reveals a very high dispersion of Fe on the mesoporous silicas obtained by using the MDD method. In the UV−vis−DR spectra of the Cr-modified materials, two intense bands at 260−280 and 360−380 nm, which correspond to the presence of Cr^{6+} as chromate (tetrahedral coordination),[33] are observed. Moreover, the very weak band at 450−470 nm, ascribed to chromate ions, is detected. Since this symmetry is forbidden in the T_d coordination, it should be assumed that chromates are grafted on the surface of silica support.[34] The appearance of Cr^{6+} in the samples obtained by the molecular design dispersion method followed by calcination and the absence of bands characteristic of Cr^{3+} in the octahedral symmetry shows that a total oxidation of Cr^{3+} cations occurred during the thermal treatment. The spectra of the Cu-containing samples consist of at least three maxima attributed to the presence of Cu^{2+} species on the sample surface. The band centered at 260 nm can be attributed to the charge transfer between mononuclear Cu^{2+} and oxygen, whereas the band around 340−360 nm corresponds to the presence of $[Cu-O-Cu]_n$-type clusters over the support surface.[35−37] Furthermore, the band observed in the region between 530 and 800 nm can be attributed to the d−d transition of Cu with octahedral environment in CuO.[38,39] The high intensity of this band reveals that the Cu-modified samples possess a relatively high amount of Cu^{2+} bulky CuO species. This effect should be attributed to the tendency to the formation of clusters by isolated Cu^{2+} during the thermal treatment at elevated temperatures. However, the formed crystallites of CuO have to be rather small, because no separate phase of copper oxide was detected in the XRD experiments (not shown).

Conclusion

The molecular designed dispersion (MDD) method can be used for grafting of acetylacetonate complex of transition metals (Cr, Fe, Cu) on the surface of mesoporous silicas. After the treatment of MCM-48, SBA-15, MCF, and MSU materials with the $Cu(acac)_2$, $Cr(acac)_3$, and $Fe(acac)_3$ complexes in a toluene solution, characteristic bands for the acetylacetonate ligands appeared in the FTIR spectra of the modified samples. The position of bands, especially $\nu_s(C-O)_{ring}$ and $\nu_{as}(C-O)_{ring}$, was affected by the nature of the central metal ion and by the type of support. Moreover, the intensity of the band at 3745 cm^{-1}, characteristic for the isolated hydroxyl group, decreased suggesting a partial disappearance of free surface OH groups.

The mechanism of interaction between the acac complexes and the support surface was elucidated by the calculation of the *R* parameter value. In the case of the MCM-48, SBA-15, and MCF samples, the deposition of metal acetylacetonate complex took place by a formation of hydrogen bonding (for $Cu(acac)_2$ and $Cr(acac)_3$) or the ligand exchange mechanism (for $Fe(acac)_3$). The *R*-values determined for the modified MSU samples suggest the formation of covalent $Me-O_{support}$ bonds for all the acac complexes.

The modification of the studied mesoporous silicas with acetylacetonate complexes did not result in a significant decrease of surface area and pore volume of the calcined materials. However, differences in textural parameters cause a limitation in the metal oxide loading in the narrow-pore MCM-48 support. The results of UV−vis−DR studies reveal that the thermal treatment of the mesoporous silicas modified with the metal acetylacetonate complexes leads to the formation of transition metal oxides dispersed on the support surface. The highest dispersion of metal was achieved for the Fe-containing materials. In the case of Cr-modified samples oxidation of Cr^{3+} to Cr^{6+} proceeded during the calcination in oxygen-containing atmosphere.

Acknowledgment. The authors thank the Ministry of Flanders and the Polish Ministry of Scientific Research and Information Technology for financial support in the frame of a bilateral Flemish-Polish project for 2004−2005.

References and Notes

(1) Kresge, C. T.; Leonowicz, M. E.; Roth, W. J.; Vartuli, J. C.; Beck, J. S. *Nature* **1992**, *359*, 710.
(2) Beck, J. S.; Vartuli, J. C.; Roth, W. J.; Leonowicz, M. E.; Kresge, C. T.; Schmitt, K. T.; Chu, C. T. W.; Olson, D. H.; Sheppard, E. W.; McCullen, S. B.; Higgins, J. B.; Schlenker, J. L. *J. Am. Chem. Soc.* **1992**, *114*, 10834.
(3) Collart, O.; Van Der Voort, P.; Vansant, E. F.; Desplantier, D.; Galarneau, A.; Di Renzo, F.; Fajula, F. *J. Phys. Chem. B* **2001**, *105*, 12771.
(4) Van Der Voort, P.; Mathieu, M.; Mees, F.; Vansant, E. F. *J. Phys. Chem. B* **1998**, *102*, 8847.
(5) Wienmeyer, M.; Anwander, R. *Chem. Mater.* **2002**, *14*, 1827.
(6) Zhao, D.; Feng, J.; Huo, Q.; Melosh, N.; Frederickson, G. H.; Chmelka, B. F.; Stucky, G. D. *Science* **1998**, *279*, 548.
(7) Zhao, D.; Huo, Q.; Feng, J.; Chmelka, B. F.; Stucky, G. D. *J. Am. Chem. Soc.* **1998**, *120*, 6024.
(8) Schmidt-Winkel, P.; Lukens, W. W.; Zhao, D.; Yang, P.; Chmelka, B. F.; Stucky, G. D. *J. Am. Chem. Soc.* **1999**, *121*, 254.
(9) Lettow, J. S.; Han, Y. J.; Schmidt-Winkel, P.; Yang, P.; Zhao, D.; Stucky, G. D.; Ying, J. Y. *Langmuir* **2000**, *16*, 8291.
(10) Choi, D. G.; Yang S. M. *J. Colloid Interface Sci.* **2003**, *261*, 127.
(11) Han, Y. J.; Watson, J. T.; Stucky, G. D.; Butler, A. *J. Mol. Catal. B: Enzym.* **2002**, *17*, 1.
(12) Tanev, P. T.; Pinnavaia, T. J. *Science*, **1995**, *267*, 865.
(13) Kim, S. S.; Zhang, W.; Pinnavaia, T. J. *Science* **1998**, *282*, 1302.
(14) Zhang, W.; Pauly, T. R.; Pinnavaia, T. J. *Chem. Mater.* **1997**, *9*, 2491.
(15) White, M. G. *Catal. Today* **1993**, *18*, 73.
(16) Serp, P.; Kalck, P.; Feurer, R. *Chem. Rev.* **2002**, *102*, 3085.

(17) Taguchi, A.; Schüth, F. *Microporous Mesoporous Mater.* **2004**, *77*, 1.
(18) Van Veen, J. A. R.; Jonckers, G.; Hesselink, W. H. *J. Chem. Soc., Faraday Trans.* **1989**, *85*, 389.
(19) Kenvin, J. C.; White, M. G.; Mitchell, M. B. *Langmuir* **1991**, *7*, 1198.
(20) Lindblad, M.; Lindfors, L. P.; Suntola, T. *Catal. Lett.* **1994**, *27*, 323.
(21) Haukka, S.; Lakomaa, E. L.; Suntola, T. *Appl. Surf. Sci.* **1994**, *75*, 220.
(22) Baltes, M.; Collart, O.; Van Der Voort, P.; Vansant, E. F. *Langmuir* **1999**, *15*, 5841.
(23) Baltes, M.; Van Der Voort, P.; Collart, O.; Vansant, E. F. *J. Porous Mater.* **1998**, *5*, 317.
(24) Collart, O.; Van Der Voort, P.; Vansant, E. F.; Gustin, E.; Bouwen, A.; Schoemaker, D.; Ramachandra Rao, R.; Weckhuysen, B. M.; Schoonheydt, R. A. *Phys. Chem. Chem. Phys.* **1999**, *1*, 4099.
(25) Schrijnemarkers, K.; Vansant, E. F. *J. Porous Mater.* **2001**, *8*, 83.
(26) Weckhuysen, B. M.; Ramachandra Rao, R.; Pelgrims, J.; Schoonheydt, R. A.; Bodart, P.; Debras, G.; Collart, O.; Van Der Voort, P.; Vansant, E. F. *Chem.*−*Eur. J.* **2000**, *6*, 2960.
(27) Van Der Voort, P.; van Welzenis, R.; de Ridder, M.; Brongersma, H. H.; Baltes, M.; Mathieu, M.; van de Ven, P. C.; Vansant, E. F. *Langmuir* **2002**, *18*, 4420.
(28) Van Bavel, E.; Cool, P.; Aerts, K.; Vansant, E. F. *J. Phys. Chem. B* **2004**, *108*, 5263.
(29) Kim, S. S.; Karkamkar, A.; Pinnavaia, T. J.; Kruk, M.; Jaroniec, M. *J. Phys. Chem. B* **2001**, *105*, 7663.
(30) Van Hoene, J.; Charles, R. G.; Hickam, W. H. *J. Phys. Chem.* **1958**, *62*, 1098.
(31) Bordiga, S.; Buzzoni, R.; Geobaldo, F.; Lamberti, C.; Giamello, E.; Zecchina, A.; Leofanti, G.; Petrini, G.; Tozzolo, G.; Vlaic, G. *J. Catal.* **1996**, *158*, 486.
(32) Pérez-Ramírez, J.; Kapteijn, F.; Brückner, A. *J. Catal.* **2003**, *218*, 234.
(33) De Rossi, S.; Casaletto, M. P.; Ferraris, G.; Cimino, A.; Minelli, G. *Appl. Catal., A* **1998**, *167*, 257.
(34) Gaspar, A. B.; Brito, J. L. F.; Dieguez, L. C. *J. Mol. Catal. A* **2003**, *203*, 251.
(35) Mendes, F. M. T.; Schmal, M. *Appl. Catal., A* **1997**, *151*, 393.
(36) Ramakrishna Prasad, M.; Kamalakar, G.; Kulkarni, S. J.; Raghavan, K. V. *J. Mol. Catal. A: Chem.* **2002**, *180*, 109.
(37) Velu, S.; Suzuki, K.; Okazaki, M.; Kapoor, M. P.; Osaki, T.; Ohashi, F. *J. Catal.* **2000**, *194*, 373.
(38) Shimokawabe, M.; Asakawa, H.; Takezawa, N. *Appl. Catal.* **1990**, *59*, 45.
(39) Centi, G.; Perathoner, S.; Biglino, D.; Giamello, E. *J. Catal.* **1995**, *151*, 75.